ISSN No: 0976-5921

Research Article

In-Silico unveiling of *Pandanus amaryllifolius* as a Cardioprotective Agent in Azithromycin-Induced Cardiotoxicity

Namit Kudatarkar[1]*, Sarvesh Havaldar[1]

1. Department of Pharmacology, KLE College of Pharmacy, Belagavi, KLE Academy of Higher Education and Research (KAHER), Belagavi, India.

Received: 09-01-2025 Accepted: 19-07-2025 Published: 30-09-2025

Abstract

This study investigates the cardioprotective potential of *Pandanus amaryllifolius* (pandan) leaf extract against azithromycin-induced cardiotoxicity, utilizing in-silico methods to uncover its key phytochemicals and mechanisms of action. The PubChem online database was used to obtain the 3D structures of all phytocompounds, which were then optimized using the MMFF94 force field. A comprehensive screening of phytochemicals using databases such as IMPPAT identified 94 compounds present in pandan leaves, of which 9 satisfied Lipinski's rule of five, indicating strong drug-likeness. Further target prediction and network analysis revealed that 40 genes were common between the cardiotoxicity-related targets and the active compounds. Pathway enrichment analysis highlighted critical signaling pathways, including HIF-1 and PI3K-Akt, as significant modulators of the protective effects. Among the identified compounds, Pandamarilactone-1 and Pandamarine exhibited particularly strong molecular interactions with key proteins such as MAPK1 and PIK3R1. These interactions were validated through molecular docking studies, which demonstrated strong binding affinities, and molecular dynamics simulations, which confirmed stable protein-ligand complexes. The findings suggest that *P. amaryllifolius* may counteract cardiotoxicity by modulating oxidative stress, reducing inflammation, and targeting key pathways involved in cardiac damage. This study positions pandan leaf extract as a promising therapeutic candidate not only for drug-induced cardiotoxicity but also for broader cardiovascular conditions, providing a foundation for further research and development.

Keywords: *Cardiotoxicity, In-silico, Pandanus amaryllifolius, Molecular docking, Molecular dynamics*

Access this article online

Website: https://ijam.co.in

DOI: https://doi.org/10.47552/ijam.v16i3.5694

Introduction

Cardiotoxicity, characterized broadly as "toxicity that affects the heart," limits the heart's ability to pump blood adequately and results from heart muscle injury (1). Cardiac disease has been a leading cause of death in India. Compared to those of European descent, CVD strikes Indians at least a decade earlier and during their most productive years. For example, 52% of CVD-related fatalities in India occur under the age of 70, compared to 23% in Western nations. Heart disease symptoms comprise rheumatic heart disease, coronary artery disease, hypertensive heart disease, cardiomyopathy, myocarditis, and arrhythmias (2). The widely administered broad-spectrum antibiotic azithromycin falls under the macrolide category. It has been approved by the Food and Drug Administration (FDA) for the treatment of respiratory tract infections and sexually transmitted infections (3).

Macrolides are among the most used families of therapeutically significant antibiotics, effective in treating infections caused by bacteria such as Staphylococcus aureus and Streptococcus pneumoniae. However, it is well recognized that macrolide antibiotics can cause arrhythmias, torsades de pointes, and lengthening of the QT interval, among other cardiotoxic consequences. These effects can be attributed to oxidative stress caused by mitochondrial damage, altered hERG K+ conductance in heart cardiomyocytes, and apoptosis signaling triggered by the release of cytochrome c from heart mitochondria into the cardiomyocyte cytosol (4). Azithromycin, a key macrolide, was quickly repurposed for the treatment of COVID-19 (5), due to its antiviral properties and immunomodulatory effects, both when used alone or in combination with hydroxychloroquine (6). However, azithromycin has been linked to QT interval prolongation and arrhythmias (7). Evidence also suggests that it can lead to reduced heart rate, prolonged PR and QT intervals, changes in the QRS complex, and T wave abnormalities.

Pandan (*Pandanus amaryllifolius* Roxb.), a plant from the Pandanaceae family, is primarily native to Southeast Asian countries (8). The Pandanaceae family includes tropical herbaceous plants known for their aromatic fragrance, making them popular in cooking to impart a basmati-like scent to rice when cooked. Beyond its culinary uses, pandan leaves are also utilized in the perfume industry and have medicinal applications as a diuretic, cardio-tonic, anti-diabetic agent, and treatment for skin diseases (9).

*** Corresponding Author:**
Namit Kudatarkar
Department of Pharmacology, KLE College of Pharmacy, Belagavi, KLE Academy of Higher Education and Research (KAHER), Belagavi, India.
Email Id: namitkudatarkar18@gmail.com

Histochemical and preliminary phytochemical screenings have indicated the presence of primary and secondary metabolites, revealing various phytoconstituents such as alkaloids, terpenoids, flavonoids, saponins and cardiac glycosides. Numerous studies have been conducted to explore their anti-cancer, antiviral, and antidiabetic properties (8).

There has been very less research on the plant for its cardioprotective activity though it contains various valuable phytoconstituents which can contribute for cardioprotective role. As there is no validation for the cardioprotective activity of Pandanus amaryllifolius, as a result, the current work aims to establish the cardioprotective efficacy of Pandanus amaryllifolius against azithromycin induced cardiotoxicity.

Material and method

Screening of main active compounds from Pandanus amaryllifiolus

The active chemical components of P. amaryllifolius were found and extracted using data from IMPPAT (IMPPAT | IMPPAT: Indian Medicinal Plants, Phytochemistry And Therapeutics (imsc.res.in), and literature mining (10).

Druglikeness prediction

The druglikeness of the phytoconstituents was assessed using the “Lipinski’s rule of five” model through MolSoft (http://www.molsoft.com/) (11).

SuperPred for target predictions of phytochemcials

SuperPred (prediction.charite.de/subpages/target_prediction.php) is a web-based prediction server designed for identifying the Anatomical Therapeutic Chemical (ATC) codes and target predictions of compounds. By predicting the ATC codes or molecular targets of small molecules, SuperPred provides valuable insights into compounds, aiding in the drug development process. It utilizes logistic regression and Morgan fingerprints of length 2048 for this purpose (12).

Uniport for ID mapping and Gene name Retrieval

To standardize the target proteins, gene names corresponding to suspected target proteins of the active chemicals in P. amaryllifolius were found using the UniProt database (https://www.uniprot.org/) (13).

Identification of Cardiotoxicity related targets

The Gene Cards database (https://www.genecards.org/) was utilized to identify cardiotoxicity-related targets by using "Cardiotoxicity" as the keyword and selecting "Homo sapiens" as the species (14).

To identify intersections between the disease and active ingredients

The online tool Venny 2.1 (Venny 2.1.0 (csic.es)) was utilized to map the active ingredient targets and disease targets, and to create Venny diagrams. The intersection of targets between P. amaryllifolius and cardiotoxicity was identified, representing the common genes of P. amaryllifolius potentially involved in the treatment of cardiotoxicity. These intersecting targets could serve as the potential target set for P. amaryllifolius in combating cardiotoxicity (15).

Establishing a network of protein-protein interactions and identifying crucial genes

To find the possible functions of target genes, we used the STRING DB (https://stringdb.org/cgi/inp ut.pl). We created a protein-protein interaction (PPI) network diagram by importing the protein interaction data into Cytoscape v3.6.1 after specifying the protein kind as Homo sapiens. Different node sizes and colours in the PPI network represented varying levels of interaction, with larger nodes signifying more important core targets (16).

Pathway and network construction

To identify the interactions between proteins and pathways where the anticipated targets influence, a list of Gene IDs were submitted to the Search Tool for the Retrieval of Connecting Genes/Proteins (STRING v12.0) (string-db.org). The KEGG pathway database (http://genome.jp/kegg/) was used to investigate the overall pathways influenced by the gene collection. Using Cytoscape v3.6.1, the network linking drugs, targets, and pathways was built, and the edge count was used to understand biological interactions. To visualize the network, node colors were set from "low value to bright colors," and node sizes were mapped to represent "low values to small sizes” (17).

Docking analysis

Protein retrieval and preparation

The PubChem online database was used to obtain the 3D structures of all phytocompounds, which were then optimized using the MMFF94 force field. A literature review and the Research Collaboratory for Structural Bioinformatics database (https://www.rcsb.org/) were utilized to identify the proteins and their respective Protein Data Bank IDs for the PIK3R1 protein (5M6U) and MAPK1 protein (2OJJ). Protein preparation was conducted using the Protein Preparation Wizard panel in Schrödinger (2021–2). This involved removing water molecules beyond 5 Å from the heteroatom groups, creating zero bond orders for metals, assigning polar hydrogens, restoring methionine residues, and performing restrained energy minimization using the optimized potential for liquid simulation (OPLS3e) force field (18).

Ligand preparation

The Epik module was utilized to produce potential ligand states at the target pH using Schrödinger's software (2021-2) LigPrep panel. A total of one stereoisomer was produced for each ligand, and chirality was maintained for the chosen ligand. Lastly, the OPLS3e force field was used to minimize energy (18).

Grid generation

A grid was made at the binding location using Schrodinger's Glide module, which has a receptor grid creation panel. The location of the co-crystal ligand was used to determine the binding site, and a grid was then produced (19).

Molecular dynamics

Using Desmond software, a 100 ns molecular dynamics (MD) simulation was run to evaluate the complex's stability. Using a Simple Point Charge water model and periodic boundary conditions, the MD system was solvated inside a cubic box of 10Å × 10Å × 10Å. The solution was neutralized by adding Na+/Cl- counter ions. A temperature of 300K and an ambient pressure of 1.01325 bar were used for the simulation. The complex's root-mean-square deviation (RMSD) and residues' root-mean-square fluctuation (RMSF) were examined in order to assess structural stability (18,19).

Result and discussion

Screening of main active compounds from Pandanus amaryllifiolus

Total of 94 phytochemicals were screening out through literature survey and through IMPPAT database. Their canonical smiles were retrieved from Pubchem.

Druglikeness prediction

By utilization of "Lipinski's rule of five" model by using MolSoft (http://www.molsoft.com/), 9 phytochemicals were screened out who followed lipinski rule of 5.

SuperPred for target predictions of phytochemicals

The SuperPred database search identified 1,015 targets for P. amaryllifolius. Gene names for these targets were retrieved from the UniProt database, and after removing null and duplicate entries, 292 unique active ingredient targets were obtained. Meanwhile, a search in GeneCard yielded 510 cardiotoxicity-related gene targets. Mapping the 292 compound targets to the 510 cardiotoxicity genes resulted in 40 shared target genes.

Identification of Cardiotoxicity related targets

Total of 510 Gene were known to be associated with cardiotoxicity.

To identify intersections between the disease and active ingredients

Mapping the 292 compound targets to the 510 cardiotoxicity genes identified 40 overlapping target genes (Fig. 1).

Fig. 1. Common genes

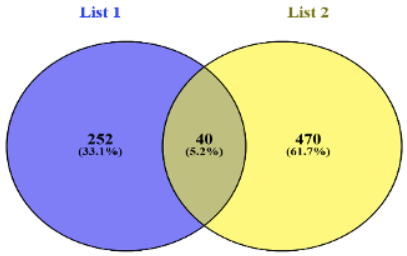

Establishing a network of protein-protein interactions and identifying crucial genes

The shared cardiotoxicity-related targets of P. amaryllifolius were imported into the STRING database to analyze their interactions. The resulting interaction network consists of 40 nodes and 176 edges (Fig. 2.). And 40 common gene were thought to modulate 105 KEGG Pathways. All the pathways were screened for their role in cardiotoxicity, and as such 17 pathways were screened out. In which the HIF-1 signaling pathway (hsa04066) scored lowest False discovery rate (FDR) of 3.47E-07 by triggering 7 gene's (MAPK1,STAT3,NOS3,TLR4,SLC2A1,PIK3R1,HIF1A), likewise AGE-RAGE signaling pathway in diabetic complications (hsa04933) scored second lowest FDR of 7.61E-05 by interacting with 5 gene's (MAPK1,MMP2,STAT3,NOS3,PIK3R1), accordingly VEGF signaling pathway (hsa04370) scored third lowest FDR of 0.00015 by interacting with 4 genes (MAPK1,NOS3,PTGS2,PIK3R1), further more Autophagy – animal, NOD-like receptor signaling pathway, IL-17 signaling pathway, Toll-like receptor signaling pathway, PI3K-Akt signaling pathway scored lowest FDR and had a role in cardiotoxicity Table 1.

Table 1: KEGG enrichment analysis and pathways

Pathway ID	Pathway name	Gene count	False discovery rate	Regulated genes
hsa04066	HIF-1 signaling pathway	7	3.47E-07	MAPK1, STAT3, NOS3, TLR4, SLC2A1, PIK3R1, HIF1A
hsa04933	AGE-RAGE signaling pathway in diabetic complications	5	7.61E-05	MAPK1, MMP2, STAT3, NOS3, PIK3R1
hsa04370	VEGF signaling pathway	4	0.00015	MAPK1, NOS3, PTGS2, PIK3R1
hsa04140	Autophagy - animal	5	0.00016	MAPK1, TBK1, CTSB, PIK3R1, HIF1A
hsa04621	NOD-like receptor signaling pathway	5	0.00042	MAPK1, TBK1, HSP90AA1, CTSB, TLR4
hsa04657	IL-17 signaling pathway	4	0.00056	MAPK1, TBK1, HSP90AA1, PTGS2
hsa04620	Toll-like receptor signaling pathway	4	0.00064	MAPK1, TBK1, TLR4, PIK3R1
hsa04151	PI3K-Akt signaling pathway	6	0.00074	MAPK1, CDK2, NOS3, HSP90AA1, TLR4, PIK3R1
hsa04068	FoxO signaling pathway	4	0.0012	MAPK1, STAT3, CDK2, PIK3R1
hsa04926	Relaxin signaling pathway	4	0.0012	MAPK1, MMP2, NOS3, PIK3R1
hsa01521	EGFR tyrosine kinase inhibitor resistance	3	0.0035	MAPK1, STAT3, PIK3R1
hsa04062	Chemokine signaling pathway	4	0.0035	MAPK1, STAT3, CXCR4, PIK3R1
hsa04020	Calcium signaling pathway	4	0.0038	NOS3, TACR1, ADRB1, CXCR4
hsa04668	TNF signaling pathway	3	0.0081	MAPK1, PTGS2, PIK3R1
hsa04611	Platelet activation	3	0.0099	MAPK1, NOS3, PIK3R1
hsa04210	Apoptosis	3	0.0119	MAPK1, CTSB, PIK3R1
hsa04217	Necroptosis	3	0.0155	STAT3, HSP90AA1, TLR4

Fig 2: Protein-protein interaction network

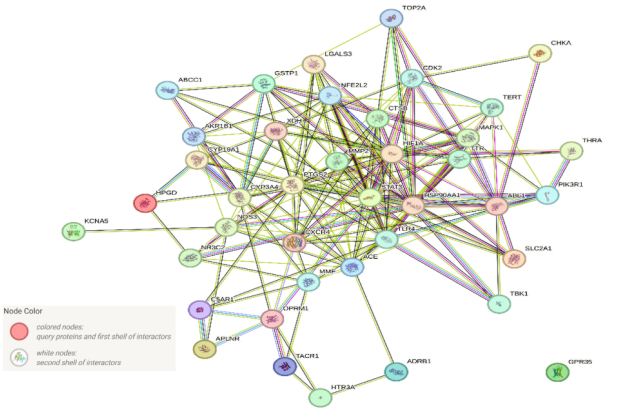

Pathway and network construction

Phytochemical gene's, pathway gene's & disease gene's all were incorporated into Cytoscape v 3.7.2, and after construction of the network it was analysed to get the highly modulated Phytochemical, Pathway and Gene. After construction and analysing the network it was concluded that Pandamarilactone-1 & Pandamarine were highly modulated and HIF-1 signaling pathway and PI3K-Akt signaling pathway were highly modulated through PIK3R1 & MAPK1 gene (Fig.3.). And as Pandamarilactonine-1 & Pandamarine were highly modulated, and these are newer phytochemicals and much study is not been carried out it was relevant to subject these two phytochemicals for Molecular dynamics.

Fig 3: Phytochemical interaction with predicted targets

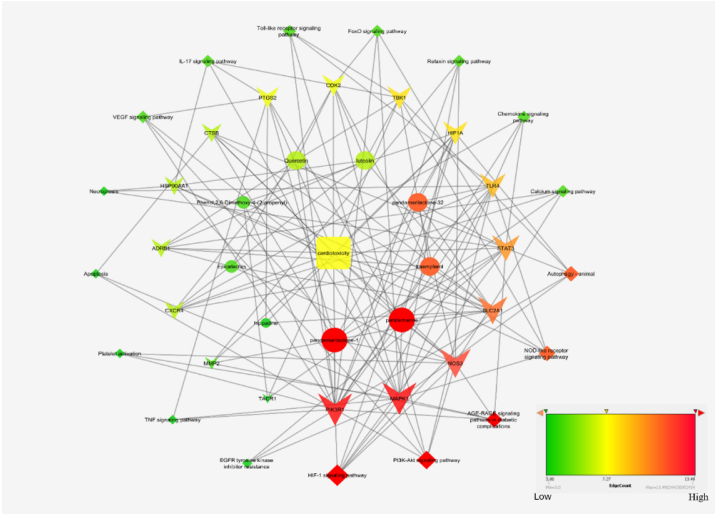

Docking analysis

The crystal structure of PIK3R1 & MAPK1 was retrieved from RCSB-PDB with PDB ID, PIK3R1 (5M6U), MAPK1 (2OJJ). All the phytoconstituents were subjected to docking with both the gene, Protein was prepared via protein preparation wizard panel of Schrodinger's (2021–2), where water beyond 5 Å from Het groups was removed, and after ligand preparation, grid generation and ligand docking results were obtained and it was found the Pandamarine and Pandamarilactone-1 showed good docking score, and shared few similar interaction as standard i.e. Pandamarilactonine-1 formed two hydrogen bond (LYS779 & VAL828) with PIK3R1 gene (Fig. 4.), whereas Pandamarine formed two hydrogen bond (LYS52 & MET106) with MAPK1 gene (Fig. 5.) both the phytochemical showed good docking score thus it was relevant to subject these two phytochemicals to molecular dynamics.

Fig 4: 2D & 3D image of Pandamarilactonine-1

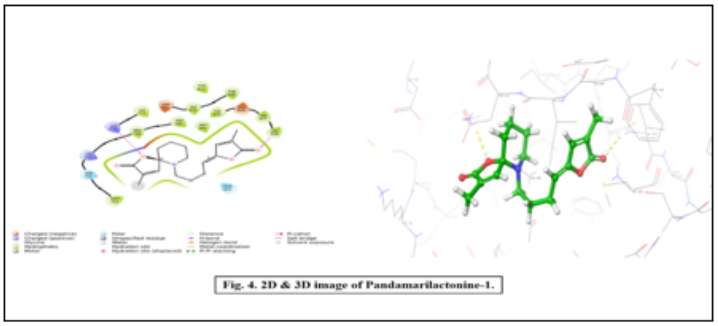

Fig 5: 2D & 3D image of Pandamarine

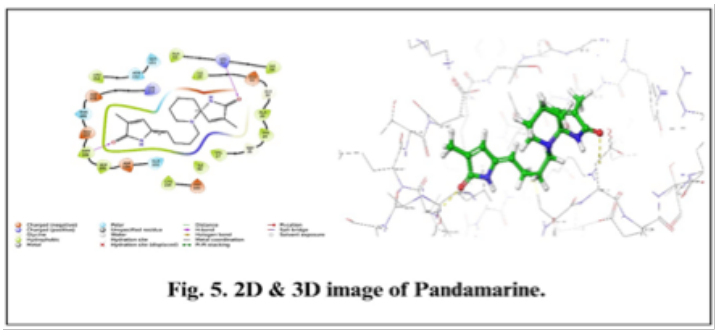

Molecular dynamics

Stability of Pandamarine with 2OJJ

The graph represents the molecular dynamics simulation of the Pandamarine ligand interacting with the protein structure identified by the PDB ID 2OJJ over a 100-nanosecond (nsec) timescale. The Protein RMSD indicates that the protein backbone remains relatively stable throughout the simulation, fluctuating between 1.8 and 2.4 Å. After an initial adjustment phase in the first 10–20 nsec, the protein's RMSD stabilizes, suggesting that it does not undergo significant conformational changes as the simulation progresses. This reflects a stable overall protein structure during ligand binding Fig. 6.

On the other hand, the Ligand RMSD shows a different trend. Initially, the ligand displays low RMSD values (~0.3 Å) during the first 40 nsec, indicating a stable binding interaction within the protein's binding pocket. However, after 40 nsec, the ligand begins to show increased fluctuations, and a sharp rise in RMSD is observed after 80 nsec, with values exceeding 10 Å. This suggests a major conformational shift or even a possible dissociation of the ligand from the binding site Fig. 6. (f).

The analysis of the RMSF graph revealed interactions between residues indexed from 29 to 165 (Fig. 6. (a)) Within this range, the protein residues interacted with the ligand. Atoms 1 and 2 exhibited minimal fluctuation, less than 2 Å, while fluctuations increased progressively from atom 3 to atom 11, with atom 11 showing the highest fluctuation of 5 Å. Beyond this, atoms 12 to 23 stabilized back to approximately 2 Å Fig. 6. (b). The increase in fluctuations can be attributed to the presence of four rotatable bonds between atoms 5 and 9.

It was observed that the MET_106 residue formed hydrogen bonds with the ligand 57% of the time Fig. 6. (c), making it the most frequent binder. This was followed by LYS_52 (17%),

ALA_33 (12%), ASP_165 (8%), GLN_103 (2%), and ASP_104 (2%). The remaining 2% of interactions were distributed among other residues Fig. 6. (d). Over the course of 100 ns, a total of 9 contacts were made between the protein and the ligand. MET_106 was responsible for the majority of these contacts, maintaining a consistent interaction throughout the entire period albeit with some intervals. This is consistent with MET_106's high hydrogen bond formation with the ligand. LYS_52 showed notable interactions between 0 to 50 ns and 60 to 80 ns, while ASP_104 had significant contacts between 30 to 80 ns Fig. 6. (e).

Fig. 6. MD simulation of Pandamarine with 2OJJ, (a) Protein RMSF, (b) Ligand RMSF, (c) Ligand protein contacts, (d) Protein ligand contacts, (e) Timeline representation of the interactions and contacts & (f) Protein ligand RMSD

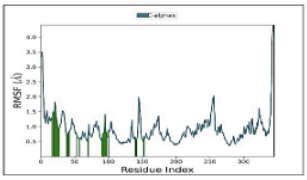

Fig 6.(a)

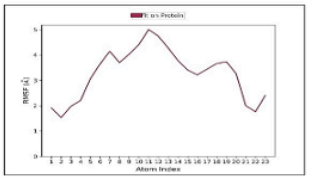

Fig 6.(b)

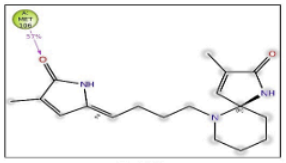

Fig 6.(c)

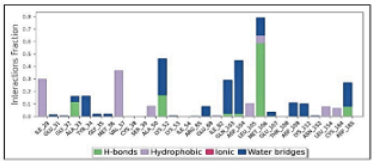

Fig 6.(d)

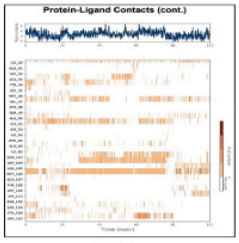

Fig 6.(e)

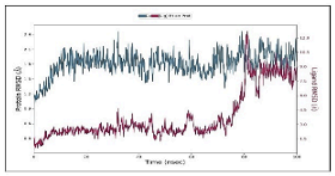

Fig 6.(f)

Stability of Pandamarilactone-1 with 5M6U

The graph illustrates the molecular dynamics simulation of the Pandamarilactone-1 ligand interacting with the protein identified by the PDB ID 5M6U over a 100-nanosecond (nsec) timescale. The Protein RMSD reveals that the protein undergoes notable structural fluctuations throughout the simulation, with values ranging between 2.0 and 4.0 Å. The protein's RMSD increases significantly in the first 20 nsec, suggesting an initial conformational adjustment, after which it oscillates between 3.0 and 4.0 Å. These fluctuations indicate that the protein experiences some degree of structural flexibility during the simulation, although it seems to stabilize somewhat after the initial phase Fig. 7.

The Ligand RMSD demonstrates a similar pattern, starting with low values (~0.5 Å) in the initial phase of the simulation, reflecting a stable binding conformation. However, it experiences an increase in RMSD over time, eventually fluctuating between 3.0 and 8.0 Å. These variations indicate that the ligand's position relative to the protein is not entirely stable, and the ligand may undergo some conformational changes or shifts in binding mode throughout the simulation Fig 7. (f).

After analyzing the RMSF graph, it was concluded that interactions were observed between residues index 708 and 911 Fig. 7. (a). Specifically, protein residues within this range interacted with the ligand.

Atom 1 to 4 exhibited minimal fluctuation, approximately 1 Å, while fluctuations increased gradually from residue 5 to 12, with residue 12 showing the highest fluctuation of 5 Å. A decrease in fluctuation was noted between residues 12 and 14, with a fluctuation of 4 Å. Between residues 14 and 19, no significant fluctuation was observed, followed by a slight increase in fluctuation, which then stabilized back to 1 Å between residues 19 and 23 Fig. 7. (b). The increase in fluctuation is attributed to the presence of four rotatable bonds between residues 5 and 9.

It was found that the VAL_828 residue formed hydrogen bonds with the ligand 96% of the time, making it the most significant contributor to ligand binding Fig. 7. (c). Following this, ASP_753 also made contact with the ligand primarily through water bridges. Additionally, THR_833, ASP_832, and SER_831 residues engaged with the ligand via water bridges Fig. 7. (d).

Over the course of 100 ns, a total of 12 contacts were made with the ligand by protein residues. VAL_828 made the most frequent contacts throughout the time period, particularly from 0 to 100 ns. This correlates with VAL_828 forming the most hydrogen bonds with the ligand. ASP_753 showed notable interactions with the ligand through water bridges primarily between 0 and 70 ns. Similarly, THR_833 and ASP_832 made significant contact with the ligand between 50 and 100 ns Fig. 7. (e).

Figure 7: MD simulation of Pandamarilactone-1 with 5M6U, (a) Protein RMSF, (b) Ligand RMSF, (c) Ligand protein contacts, (d) Protein ligand contacts, (e) Timeline representation of the interactions and contacts & (f) Protein ligand RMSD

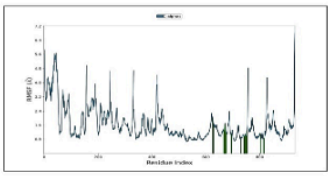

Fig 7.(a)

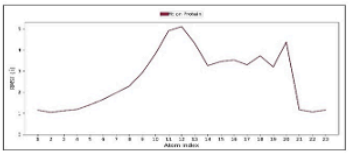

Fig 7.(b)

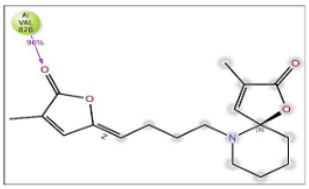

Fig 7.(c)

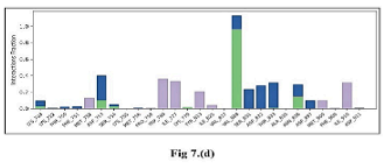

Fig 7.(d)

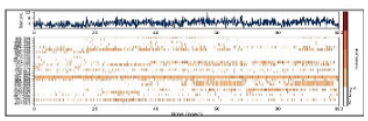

Fig 7.(e)

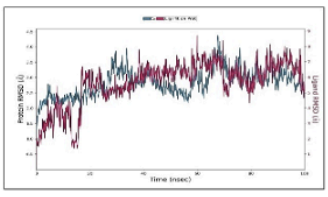

Fig 7.(f)

Discussion

The current study delves into the cardioprotective properties of *Pandanus amaryllifolius* (commonly referred to as pandan) leaf extract against azithromycin-induced cardiotoxicity, an area of increasing importance in light of rising cardiovascular diseases (CVDs) and the widespread use of azithromycin (24). CVDs

remain a leading cause of death globally, especially in regions like India, where they tend to affect younger populations more severely compared to the West. The discussion highlights the significance of addressing the side effects associated with azithromycin, a macrolide antibiotic commonly used to treat respiratory infections, which saw heightened use during the COVID-19 pandemic (23). Its potential for causing QT interval prolongation and arrhythmias (26), underscores the importance of exploring new therapeutic agents to mitigate these risks. By investigating *P. amaryllifolius*, the study brings attention to a plant that, despite its known culinary and medicinal benefits, has received little scientific validation for its cardioprotective properties (25).

A key aspect of the study is the *in-silico* screening of *P. amaryllifolius* phytochemicals to identify those with potential cardioprotective activity. Through the use of databases such as IMPPAT, a total of 94 active phytochemicals were identified, and 9 compounds were deemed drug-like based on Lipinski's rule of five, indicating their potential efficacy as drug candidates. The compounds were analyzed for their interaction with cardiotoxicity-related gene targets, and 40 common target genes were identified, bridging the gap between the phytochemicals of *P. amaryllifolius* and the mechanisms underlying cardiotoxicity. This finding is significant as it provides a molecular basis for understanding how *P. amaryllifolius* may exert its cardioprotective effects.

Moreover, the protein-protein interaction (PPI) network analysis revealed that *P. amaryllifolius* influences several critical signaling pathways involved in cardiotoxicity. Notably, pathways such as the HIF-1 signaling pathway and PI3K-Akt signaling pathway were highlighted, both of which play essential roles in heart function and the cellular response to stress (20). Additionally, the study identified pathways like the AGE-RAGE signaling pathway (22), commonly associated with diabetic complications, and the VEGF signaling pathway (21), which is linked to vascular health and oxidative stress. The identification of these pathways underscores the broad therapeutic potential of *P. amaryllifolius*, suggesting that it may help combat not only drug-induced cardiotoxicity but also conditions related to oxidative damage and inflammation in cardiovascular diseases.

Among the phytochemicals identified, Pandamarilactone-1 and Pandamarine emerged as the most modulated compounds in their interactions with cardiotoxicity-related proteins. Molecular docking studies demonstrated that these compounds showed strong binding affinities with the PIK3R1 and MAPK1 proteins, two key players in cardiac function. Pandamarilactone-1, for example, was found to form hydrogen bonds with PIK3R1, while Pandamarine formed similar interactions with MAPK1. These results suggest that both compounds have the potential to stabilize critical proteins involved in heart function, which may help mitigate the damaging effects of azithromycin-induced cardiotoxicity. The favourable docking scores further solidify their potential as lead compounds for future drug development targeting cardio protection.

To support these findings, the study utilized molecular dynamics simulations over a 100-nanosecond (ns) timescale to evaluate the stability of the protein-ligand complexes formed by Pandamarilactone-1 and Pandamarine. The simulation results revealed that the protein backbones remained relatively stable, while the ligands showed minor fluctuations, reflecting the dynamic nature of the protein-ligand interactions. Notably, key residues like MET_106 and LYS_52 were identified as critical contributors to maintaining the stability of the protein-ligand complex for Pandamarine, while VAL_828 and ASP_753 played significant roles in stabilizing the Pandamarilactone-1 complex. These results further strengthen the case for the cardioprotective potential of these phytochemicals.

The discussion concludes that *P. amaryllifolius* shows great promise as a source of cardioprotective agents, particularly Pandamarilactone-1 and Pandamarine. Their interactions with key signaling pathways and proteins involved in cardiotoxicity highlight their potential as natural remedies for mitigating the cardiotoxic effects of drugs like azithromycin. However, the study also acknowledges the limitations of in silico analyses and the need for further validation through in vivo and clinical studies. Future research should explore the biological efficacy of these compounds in living systems and investigate their potential synergistic effects with existing cardioprotective drugs.

In summary, this study lays the foundation for further exploration of *P. amaryllifolius* as a natural source of cardioprotective compounds. By identifying key phytochemicals and their interactions with molecular targets involved in cardiotoxicity, the research opens new avenues for developing plant-based solutions to address heart-related health issues. Given the ongoing concerns surrounding drug-induced cardiotoxicity, especially in light of the COVID-19 pandemic, these findings are both timely and relevant, offering a potential pathway for safer therapeutic strategies to protect the heart from harmful side effects.

Conclusion

In conclusion, this study has successfully identified Pandanus amaryllifolius as a highly promising source of cardioprotective compounds. Among the phytochemicals analyzed, Pandamarilactone-1 and Pandamarine have emerged as standout candidates with significant potential for further exploration. These compounds have demonstrated the ability to target critical signaling pathways and stabilize key proteins essential for maintaining optimal heart function. By doing so, they offer a novel and natural approach to mitigating the cardiotoxic effects induced by azithromycin, a widely used antibiotic. Cardiovascular diseases and drug-induced cardiotoxicity remain persistent global health challenges, contributing to significant morbidity and mortality rates worldwide. The findings of this research provide a foundation for the development of plant-based therapeutic strategies that not only safeguard heart health but also address the pressing need for safer pharmacological interventions. Furthermore, the potential of Pandanus amaryllifolius phytochemicals to modulate complex biochemical pathways underscores their versatility as candidates for integrative medicinal approaches. By highlighting the cardioprotective effects of natural compounds, this study paves the way for innovative solutions that align with the growing emphasis on alternative and sustainable healthcare options. It also sets the stage for future investigations into the mechanisms underlying these compounds' protective effects, clinical trials to validate their efficacy, and their eventual application in reducing the risks associated with essential but potentially cardiotoxic medications like azithromycin. As the quest for safe and effective remedies continues, Pandanus amaryllifolius stands out as a beacon of hope in advancing cardiovascular health through nature-inspired solutions.

Acknowledgements

The authors extend their heartfelt gratitude to the Department of Pharmacology and Toxicology & Department of Pharmaceutical chemistry at KLE College of Pharmacy, Belagavi, for their

invaluable technical support and for fostering a conducive research environment.

Declaration of competing interest

The authors declare no conflict of interest related to this manuscript.

References

1. Maria F, Mircea C, Dragos V. Chemotherapy-induced Cardiotoxicity. Maedica. 2013 Mar;8(1):59–67.
2. Dorairaj P, Panniyammakal J, Ambuj R. Cardiovascular Diseases in India: Current Epidemiology and Future Directions. Circulation . 2016;133(16):1605–20.
3. Basma S M, Noha A S , Ghada A K, Gamal A A, Omayma M M. Protective effect of Rosuvastatin on Azithromycin induced cardiotoxicity in a rat model. Life Sci 2021;269:119099.
4. Ahmad S , Sadaf E, Enayatollah S, Parvaneh N, Negar P K, Jalal P. Toxicity of macrolide antibiotics on isolated heart mitochondria: a justification for their cardiotoxic adverse effect. Xenobiotica. 2016;46(1):82–93.
5. Iwein G, Wim J, Peter V, Robin V. Rationale for azithromycin in COVID-19: an overview of existing evidence. BMJ Open Respir Res. 2021;8(1):e000806.
6. Julien A, Marion L B, Isabelle D, Priscilla J, Clara R, Manon B, Nathalie W, Jean M R, Philippe C, Bernard L S, Didier R. In vitro testing of combined hydroxychloroquine and azithromycin on SARS-CoV-2 shows synergistic effect. Microb Pathog. 2020;145:104228.
7. Yizhou L, Rai Z, Jules C H, Henggui Z. In silico investigation of pro-arrhythmic effects of azithromycin on the human ventricle. Biochem Biophys Rep. 2021;27:101043.
8. Winny R, Kalpana R. Chemical Constituents and Post-Harvest Prospects of *Pandanus amaryllifolius* Leaves: A Review. Food Rev Int. 2010;26(3):230–45.
9. Ampa J, Panvipa K. Antioxidant Activity of *Pandanus amaryllifolius* Leaf and Root Extract and its Application in Topical Emulsion. Trop J Pharm Res. 2016;12(3):425–31.
10. Rageshree C, Kankana T, Anwesha M, Sanghati T. In-vitro and in-silico therapeutic investigation and biochemical characterization of Mangifera indica: A flowering plant. J Med Plants Stud. 2024;12(4):256–71.
11. Pukar K, Basava M P, Bijendra K M, Yadu N D, Taza D. Network pharmacology-based assessment to elucidate the molecular mechanism of anti-diabetic action of Tinospora cordifolia. Clin Phytoscience. 2019;5(1):35.
12. Sabrin R I,Abdelsattar M O, Alaa A B, Reem M D, Ahmad O N, Diena M A, Shaimaa G M, Gamal A M. Thiophenes—Naturally Occurring Plant Metabolites: Biological Activities and In Silico Evaluation of Their Potential as Cathepsin D Inhibitors. Plants. 2022;11(4):539.
13. Laigen Z, Xiaoqing S, Zhengquan H, Jun M, Wei M, Liang D, Li Z, Runlin X, Peimin W. Network Pharmacology Approach to Uncover the Mechanism Governing the Effect of Radix Achyranthis Bidentatae on Osteoarthritis. BMC Complement Med Ther. 2020;20(1):121.
14. Akhtar A, YoungJoon P, Jeonghoon L, Hyo J A, Jong S J, Jong H L, Jaeki C, Dong K K, Bonhyuk G, Yeon C P, Kang H L, Shin S, Wonnam K. In Vitro Study of Licorice on IL-1β-Induced Chondrocytes and In Silico Approach for Osteoarthritis. Pharmaceuticals. 2021;14(12):1337.
15. Aysegul Y,Seyhan T, Ayriana B S, Can T. Unraveling the Influence of Escherichia coli Strains on Gene Expression in Colorectal Cancer Cells through in Silico Analysis. Lokman Hekim Health Sci. 2023;153–60.
16. Jin R L, Yue H, Ping L,Zi Y C, Qi Q C,Shi W. Mechanism of Cordyceps sinensis in atherosclerosis treatment based on network pharmacology and molecular docking analysis. Precis Med Res. 2023;5(2):10.
17. Jiaqin L, Taoli S, Sa L, Jian L, Senbiao F, Shengyu T, Yucheng Z, Bikui Z, Wenqun L. Dissecting the molecular mechanism of cepharanthine against COVID-19, based on a network pharmacology strategy combined with RNA-sequencing analysis, molecular docking, and molecular dynamics simulation. Comput Biol Med. 2022;151:106298.
18. Sanjay R. U, Nayeem A. K, Vishal S. P, Dhanashree P, Jagadeesh D Computational and experimental pharmacology reveals hepatoprotective effect of Cucurbita pepo in isoniazid-induced liver cirrhosis. J Appl Pharm Sci. 2023;14(1):177-88.
19. Namit K, Sunil J, Vishal S. P, Bhaskar K. System biology and chemoinformatics approaches to decode the molecular mechanisms of Chrysin against colon cancer. J Appl Pharm Sci. 2021;
20. Fatemeh Y, Wallace H, Gholamreza K. Natural compounds against cytotoxic drug-induced cardiotoxicity: A review on the involvement of PI3K/Akt signaling pathway. Journal of Biochemical and Molecular Toxicology. 2021;35(3):e22683.
21. Marwa M M R, Maram E H, Elshymaa A H, Michael A F, Eman S M A E R, Sayed S. Phosphodiesterase inhibitor, Vinpocetine, guards against doxorubicin induced cardiotoxicity via modulation of HIF/VEGF and cGMP/cAMP/SIRT signaling pathways. Human & Experimental Toxicology. 2022;41:09603271221136209.
22. Minmin L, Lin Y, Rui W, Lin L, Yifan Z, Long L, Nuo J, Yatao H, Zhiqiang K, Frédéric F, Bei F, Fengzhong W. Stereoselective cardiotoxic effects of metconazole on zebrafish based on AGE-RAGE signalling pathway. Science of The Total Environment. 2024;912:169304.
23. Janet S, Paola M C, Salvatore C, Gabriele P, Gaetano C, Gianluca T. Azithromycin in COVID-19 patients: pharmacological mechanism, clinical evidence and prescribing guidelines. Drug safety. 2020;43:691-8.
24. Bharat D, Manoli V, Erjian W, Joanne L, Brian C. Clinical pharmacology perspectives on the antiviral activity of azithromycin and use in COVID19. Clinical Pharmacology & Therapeutics. 2020;108(2):201-11.
25. Suttipalin S, Plykaeow C, Suttasinee S. Antioxidant Anti-Cancer and Antimicrobial Activities of Ethanol Pandanus amaryllifolius Roxb. leaf extract (In Vitro)-A potential medical application. Journal of International Dental & Medical Research. 2018;11(2):383-89
26. Young C, Hong S L, Dahee C, Jung G C, Dukyong Y. Risk evaluation of azithromycin induced QT prolongation in real world practice. BioMed research international. 2018;2018(1):1574806.

*****